1
2
3
4
5
6
7
8
9 Latent functional connectivity underlying multiple brain states
10
11
12 Ethan M. McCormick *[†a,b], Katelyn L. Arnemann [†a], Taku Ito [a,c], Stephen J. Hanson [d], &
13 Michael W. Cole [a]
14
15 [†]denotes equal authorship
16
17 [a] Center for Molecular and Behavioral Neuroscience, Rutgers University, Newark, New Jersey; [b]
18 Department of Psychology and Neuroscience, University of North Carolina, Chapel Hill, United
19 States; [c] Yale University School of Medicine, Yale University, New Haven, Connecticut; [d]
20 Rutgers University Brain Imaging Center, Newark, New Jersey.
21
22
23
24
25
26
27
28
29
30
31
32
33
34
35
36
37
38
39
40
41
42 *corresponding author
43 Ethan M. McCormick
44 Center for Molecular and Behavioral Neuroscience,
45 Rutgers University
46 197 University Avenue, Newark, NJ 07102
47 ethan.mccormick@rutgers.edu

Abstract

48

49   Functional connectivity (FC) studies have predominantly focused on resting state, where

50   ongoing dynamics are thought to primarily reflect the brain's intrinsic network architecture,

51   which is thought to be broadly relevant to brain function because it persists across brain states.

52   However, it is unknown whether resting state is the optimal state for measuring intrinsic FC. We

53   propose that latent FC, reflecting patterns of connectivity shared across many brain states, may

54   better capture intrinsic FC relative to measures derived from resting state alone. We estimated

55   latent FC in relation to 7 highly distinct task states (24 task conditions) and resting state using

56   fMRI data from 352 participants from the Human Connectome Project. Latent FC was estimated

57   independently for each connection by applying leave-one-task-out factor analysis on the state FC

58   estimates. Compared to resting-state connectivity, we found that latent connectivity improves

59   generalization to held-out brain states, better explaining patterns of both connectivity and task-

60   evoked brain activity. We also found that latent connectivity improved prediction of behavior,

61   measured by the general intelligence factor psychometric g. Our results suggest that patterns of

62   FC shared across many brain states, rather than just resting state, better reflects general, state-

63   independent connectivity. This affirms the notion of "intrinsic" brain network architecture as a

64   set of connectivity properties persistent across brain states, providing an updated conceptual and

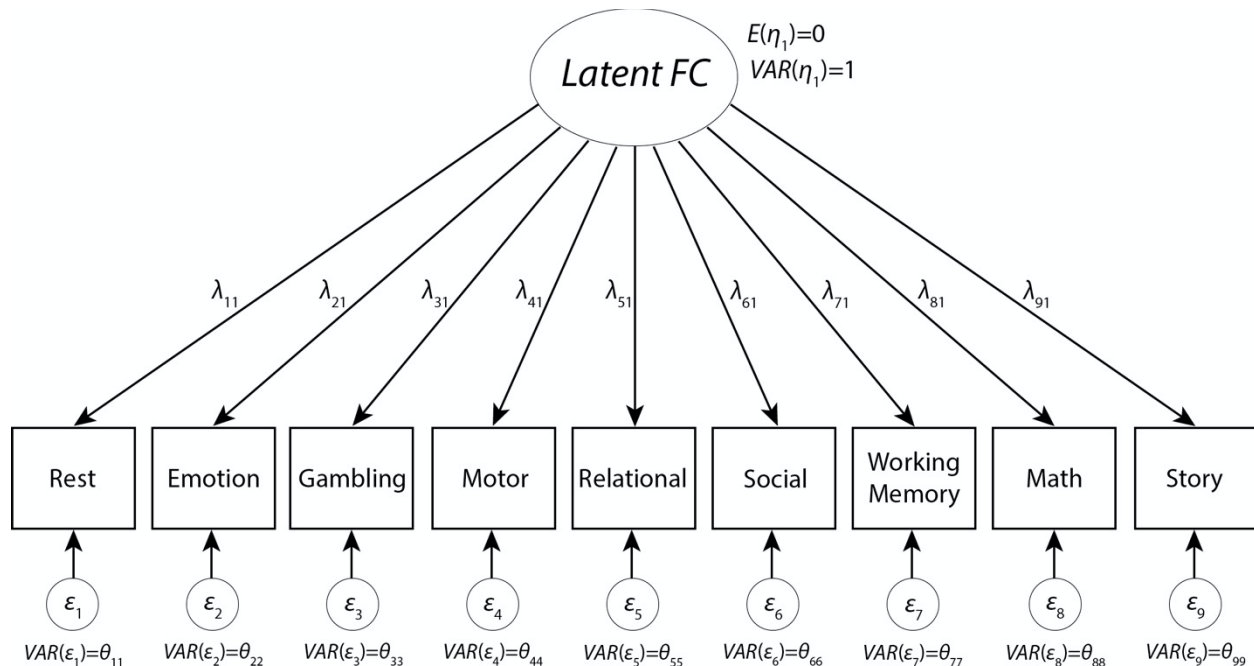65   mathematical framework of intrinsic connectivity as a latent factor.

66

Introduction

67

68   A major goal in cognitive neuroscience in recent years has been to move away from

69   characterizing brain activation and connectivity in specific task states towards understanding

70   "intrinsic" or context-free brain activity. Such activity reflects the more than 95% of metabolic

71   brain activity that remains unchanged across cognitive demands (Raichle, 2006). This ongoing

72   brain activity persists across states and is not attributable to external stimuli or task demands.

73   Efforts to understand intrinsic function have focused primarily on statistical associations between

74   brain activity time series (functional connectivity; FC) during the resting state (Fox & Raichle,

75   2007), which has revealed an intrinsic brain functional network architecture that recapitulates

76   patterns of task-evoked brain activity (Cole, Ito, Bassett, & Schultz, 2016; Smith et al., 2009) and

77   structural connectivity (Honey et al., 2009). Despite its importance for understanding brain

78   function, many uncertainties remain on how to best estimate intrinsic FC. While some efforts have

79   focused on the need to obtain longer resting-state scans (Anderson, Ferguson, Lopez-Larson, &

80   Yurgelun-Todd, 2011; M. Elliott et al., 2019; Hacker et al., 2013; Laumann et al., 2015) more

81   recent approaches have highlighted advantages of combining resting-state and task data to analyze

82   intrinsic activity.

83   This second set of approaches leverages functional data across different task (and rest)

84   scans in order to improve the reliability of FC estimates and their predictive utility (M. Elliott et

85   al., 2019) Because of the relatively high stability of FC networks across task states (Cole, Bassett,

86   Power, Braver, & Petersen, 2014; Gratton et al., 2018; Krienen, Yeo, & Buckner, 2014),

87   combining data across task runs aims to distinguish what is common across a larger set of brain

88   states. What is common therefore reflects the intrinsic patterns of covariance in the brain, while

89   variation between different brain states is treated as noise in the combined data. However, this

90   work largely relies on averaging data from multiple scans together (M. Elliott et al., 2019). While

91   this approach has been shown to be useful, and has the advantage of simplicity, there are potential

92   theoretical limitations to such an approach that may limit its generalizability. Given its ubiquity

93   and close-formed, arithmetic solution, the average is rarely thought of as a formal statistical model.

94   However, recent work (McNeish & Wolf, 2020) has shown that the average can be thought of as

95   a restricted case of the more-general factor analytic model. Embedding the average in a

96   theoretically rich statistical framework is likely to offer advantages for interpretation of results

97   using this measure as well as insights into the measure itself.

98   Factor analysis has a long tradition in the behavioral sciences (Spearman, 1904; Thurstone,

99   1935) and is an invaluable tool in psychometrics and psychological measurement. Its key insight

100   is that observed measures (e.g., behavioral responses or fMRI scans) are imperfect manifestations

101   of an unobserved (i.e., latent) variable (Bollen, 2002). In the factor model, observed indicators ($y_{i,t}$;

102   i = individual, t = task state) are modeled as dependent on the underlying latent factor (η; Figure

103   1). Variability in the indicators is partitioned into common variance (transmitted through the factor

104   loading matrix, Λ) and unique variance (ε_t). In this model, latent FC represents an unmeasured,

105   underlying brain state that is common to all observed brain states (i.e., the indicators: resting state,

106   motor task, etc.), but we also explicitly model additional variance that is only found in each

107   individual task state through the error terms. Factor loadings for the individual task states (e.g., λ_{11}

108   for Rest) in this single-factor model can be interpreted as the proportion of variance explained in

109   each task state by latent FC (similar to R^2 in regression).

$E(\eta_1)=0$
$VAR(\eta_1)=1$

Latent FC

λ_{11} λ_{21} λ_{31} λ_{41} λ_{51} λ_{61} λ_{71} λ_{81} λ_{91}

| Rest | Emotion | Gambling | Motor | Relational | Social | Working Memory | Math | Story |

ε_1 ε_2 ε_3 ε_4 ε_5 ε_6 ε_7 ε_8 ε_9

$VAR(\varepsilon_1)=\theta_{11}$ $VAR(\varepsilon_2)=\theta_{22}$ $VAR(\varepsilon_3)=\theta_{33}$ $VAR(\varepsilon_4)=\theta_{44}$ $VAR(\varepsilon_5)=\theta_{55}$ $VAR(\varepsilon_6)=\theta_{66}$ $VAR(\varepsilon_7)=\theta_{77}$ $VAR(\varepsilon_8)=\theta_{88}$ $VAR(\varepsilon_9)=\theta_{99}$

Figure 1. Factor Model. *A set of indicators (e.g., Rest, the Motor task, etc.) are modeled being composed of shared underlying variance, as represented by the latent factor (i.e., Latent FC), and unique task-state variance (in the errors). Factor loadings (λ) represent the percent variance in each task state that is explained by the underlying Latent FC.*

As can be seen in Figure 1, the factor analysis model of latent FC is a parameter-rich model that allows for differentially weighted relationships between the underlying latent connectivity and measured connectivity in each specific state. What McNeish and Wolf (2020) showed, however, is that the average can be recovered using this model by setting all factor loadings (λ) equal to 1 and the unique variances to 0. This recast of the average as a special case of the factor model not only has the advantage of making the assumptions of the average clearer, but it enables a formal test of those assumptions. For instance, by setting all factor loadings equal, the average assumes that each observed FC state is equally (and positively) related to the underlying latent FC. If we want to relax that assumption, the factor analytic model can be used to compute unique optimally weighted values for each factor loading, which suggests that some observed states may be better (or worse) reflections of underlying latent FC. Indeed, factor loadings may take on negative values,

127   which implies that an observed indicator is anti-correlated with the underlying latent FC. However,

128   if the assumption of equal, positive weighting is indeed an appropriate assumption, freely

129   estimated factor loadings will converge towards equal values and approximate the average. In

130   other words, the flexibility of the full factor loading does not preclude the average, but instead

131   offers a broader range of possibility for deriving a measure of latent FC in heterogeneous data and

132   can be used to test the validity of the average FC assumption of equal positive factor loadings

133   across brain states.

134   Here, we test the reliability of a factor analytic framework for modeling state-general brain

135   connectivity – "intrinsic" FC that generalizes across a variety of brain states. First, we

136   hypothesized that latent FC reflects a positive manifold (analogous to the positive correlations

137   across intelligence tests in general intelligence research; (Kovacs & Conway, 2016)), where all

138   state-specific connectivity values are positively correlated with each other and so load positively

139   onto the underlying latent variable. This would confirm that a single common intrinsic functional

140   network architecture exists across conscious brain states. We further hypothesized that by

141   combining information across task states, such as in the factor model, a more reliable measure of

142   "intrinsic" connectivity can be estimated than when using resting state data alone (the current field

143   standard). This would suggest that resting-state FC is not necessarily the best state for estimating

144   intrinsic FC, especially if resting state does not load higher on the latent variable than other states.

145   In testing these hypotheses, we developed an analytic framework for estimating state-general,

146   latent FC in whole-brain functional data. Using multi-task fMRI data from the Human Connectome

147   Project (HCP), we compare the ability of latent and resting-state FC to predict task-evoked

148   activation and task-state FC for held-out brain states, as well as to explain individual differences

149   in psychometric "g" (a measure of human intelligence derived with a similar factor analytic

150   model). Results demonstrate the promise of the latent variable approach in functional

151   neuroimaging, particularly for the estimation of intrinsic FC that generalizes beyond specific brain

152   states (e.g., rest). Finally, we demonstrate the relationship between freely estimated latent FC and

153   the simpler average FC approach and discuss the theoretical advantages of casting both methods

154   in the latent variable framework for future work.

155

156   **Methods**

157   For clarity, portions of the text in this section are from our prior publication using the same

158   dataset and some identical analysis procedures: Ito et al. (2020).

159   **Participants**

160   Data in the present study were collected as part of the Washington University-Minnesota

161   Consortium of the Human Connectome Project (HCP) (Van Essen et al., 2013). A subset of data (

162   n = 352) from the HCP 1200 release was used for empirical analyses. Specific details and

163   procedures of subject recruitment can be found in Van Essen et al. (2020). The subset of 352

164   participants was selected based on: quality control assessments (i.e., any participants with any

165   quality control flags were excluded, including 1) focal anatomical anomaly found in T1w and/or

166   T2w scans, 2) focal segmentation or surface errors, as output from the HCP structural pipeline, 3)

167   data collected during periods of known problems with the head coil, 4) data in which some of the

168   FIX-ICA components were manually reclassified; exclusion of high-motion participants

169   (participants that had any fMRI run in which more than 50% of TRs had greater than 0.25mm

170   framewise displacement); removal according to family relations (unrelated participants were

171   selected only, and those with no genotype testing were excluded). A full list of the 352 participants

172   used in this study will be included as part of the code release.

173   All participants were recruited from Washington University in St. Louis and the

174   surrounding area. We split the 352 subjects into two cohorts of 176 subjects: an exploratory cohort

175   (99 women) and a validation cohort (84 women). The exploratory cohort had a mean age of 29

176   years of age (range=22-36 years of age), and the validation cohort had a mean age of 28 years of

177   age (range=22-36 years of age). All subjects gave signed, informed consent in accordance with the

178   protocol approved by the Washington University institutional review board.

179   **Scan Acquisition**

180   Whole-brain multiband echo-planar imaging acquisitions were collected on a 32-channel

181   head coil on a modified 3T Siemens Skyra with TR=720 ms, TE=33.1 ms, flip angle=52º,

182   Bandwidth=2,290 Hz/Px, in-plane FOV=208x180 mm, 72 slices, 2.0 mm isotropic voxels, with a

183   multiband acceleration factor of 8. Data for each subject were collected over the span of two days.

184   On the first day, anatomical scans were collected (including T1-weighted and T2-weighted images

185   acquired at 0.7 mm isotropic voxels) followed by two resting-state fMRI scans (each lasting 14.4

186   minutes) and ending with a task fMRI component. The second day consisted of first collecting a

187   diffusion imaging scan, followed by a second set of two resting-state fMRI scans (each lasting

188   14.4 minutes), and again ending with a task fMRI session.

189   Each of the seven tasks was collected over two consecutive fMRI runs. The seven tasks

190   consisted of an emotion cognition task, a gambling reward task, a language task, a motor task, a

191   relational reasoning task, a social cognition task, and a working memory task. Briefly, the emotion

192   cognition task required making valence judgements on negative (fearful and angry) and neutral

193   faces. The gambling reward task consisted of a card guessing game, where subjects were asked to

194   guess the number on the card to win or lose money. The language processing task consisted of

195   interleaving two language conditions, which involved answering questions related to a story

196 presented aurally, and a math condition, which involved basic arithmetic questions presented

197 aurally. Note that we treated the two language task conditions as separate tasks, given the highly

198 distinct nature of the conditions (other than that they were presented aurally). The motor task

199 involved asking subjects to either tap their left/right fingers, squeeze their left/right toes, or move

200 their tongue. The reasoning task involved asking subjects to determine whether two sets of objects

201 differed from each other in the same dimension (e.g., shape or texture). The social cognition task

202 was a theory of mind task, where objects (squares, circles, triangles) interacted with each other in

203 a video clip, and subjects were subsequently asked whether the objects interacted in a social

204 manner. Lastly, the working memory task was a variant of the N-back task. Further details on the

205 resting-state fMRI portion can be found in (Smith et al., 2013), and additional details on the task

206 fMRI components can be found in (Barch et al., 2013) .

207 **Behavior: Data**

208 To assess generalized intelligence (g), we drew 11 measures of cognitive ability from the

209 HCP dataset, which are derived from the NIH Toolbox for Assessment of Neurological and

210 Behavioral function (http://www.nihtoolbox.org; (Gershon et al., 2013) and the Penn

211 computerized neurocognitive battery (Gur et al., 2010). Tasks included: picture sequence memory;

212 dimensional card sort; flanker attention and inhibitory control; the Penn Progressive Matrices; oral

213 reading recognition; picture vocabulary; pattern completion processing speed; variable short Penn

214 line orientation test; Penn word memory test (number correct and median reaction time as separate

215 variables]) and list sorting. For all measures, the age-unadjusted score was used where applicable.

216 For complete information regarding all measures, see the descriptions in the Cognition Category

217 of the HCP Data Dictionary

218   (https://wiki.humanconnectome.org/display/PublicData/HCP+Data+Dictionary+Public-

219   +Updated+for+the+1200+Subject+Release).

Behavior: Factor analysis model of psychometric 'g'

221   We then derived a general factor of intelligences using a multiple-indicator latent factor

222   model. We approach the factor model using a confirmatory factor analysis (CFA) approach with a

223   unitary factor underlying all individual cognitive tasks. Factor loadings were estimated using the

224   *psych* R package (Revelle, 2017). Factor scores were computed using the regression method

225   (Thurstone, 1935) to obtain manifest variables for prediction.

fMRI: Preprocessing

227   Minimally preprocessed data for both resting-state and task fMRI were obtained from the

228   publicly available HCP data. Minimally preprocessed surface data was then parcellated into 360

229   brain regions using the Glasser atlas (Glasser et al., 2016). We performed additional preprocessing

230   steps on the parcellated data for resting-state fMRI and task state fMRI to conduct neural

231   variability and FC analyses. This included removing the first five frames of each run, de-meaning

232   and de-trending the time series, and performing nuisance regression on the minimally preprocessed

233   data (Ciric et al., 2017) . Nuisance regression removed motion parameters and physiological noise.

234   Specifically, six primary motion parameters were removed, along with their derivatives, and the

235   quadratics of all regressors (24 motion regressors in total). Physiological noise was modeled using

236   aCompCor on time series extracted from the white matter and ventricles (Behzadi, Restom, Liau,

237   & Liu, 2007) . For aCompCor, the first 5 principal components from the white matter and

238   ventricles were extracted separately and included in the nuisance regression. In addition, we

239   included the derivatives of each of those components, and the quadratics of all physiological noise

240   regressors (40 physiological noise regressors in total). The nuisance regression model contained a

241 total of 64 nuisance parameters. This was a variant of previously benchmarked nuisance regression

242 models reported in (Ciric et al., 2017) .

243 We excluded global signal regression (GSR), given that GSR can artificially induce

244 negative correlations (Murphy, Birn, Handwerker, Jones, & Bandettini, 2009; Power et al., 2014),

245 which could bias analyses of whether global correlations decrease during task performance. We

246 included aCompCor as a preprocessing step here given that aCompCor does not include the

247 circularity of GSR (regressing out some global gray matter signal of interest) while including some

248 of the benefits of GSR (some extracted components are highly similar to the global signal) (Power

249 et al., 2018). This logic is similar to a recently-developed temporal-ICA-based artifact removal

250 procedure that seeks to remove global artifact without removing global neural signals, which

251 contains behaviorally relevant information such as vigilance (Glasser et al., 2018; Wong, Olafsson,

252 Tal, & Liu, 2013). We extended aCompCor to include the derivatives and quadratics of each of

253 the component time series to further reduce artifacts. Code to perform this regression is publicly

254 available online using python code (version 2.7.15) (https://github.com/ito-

255 takuya/fmriNuisanceRegression). Following nuisance regression, the time series for each run

256 (task-state and rest-state) were z-normalized such that variances across runs would be on the same

257 scale (i.e., unit variance).

258 Task data for task FC analyses were additionally preprocessed using a standard general

259 linear model (GLM) for fMRI analysis. For each task paradigm, we removed the mean evoked

260 task-related activity for each task condition by fitting the task timing (block design) for each

261 condition using a finite impulse response (FIR) model (Cole et al., 2019) . (There were 24 task

262 conditions across seven cognitive tasks.) We used an FIR model instead of a canonical

263 hemodynamic response function given recent evidence suggesting that the FIR model reduces both

264   false positives and false negatives in the identification of FC estimates (Cole et al., 2019). This is

265   due to the FIR model's ability to flexibly fit the mean-evoked response across all blocks.

266   FIR modeled task blocks were modeled separately for task conditions within each of the

267   seven tasks. In particular, two conditions were fit for the emotion cognition task, where coefficients

268   were fit to either the face condition or shape condition. For the gambling reward task, one condition

269   was fit to trials with the punishment condition, and the other condition was fit to trials with the

270   reward condition. For the language task, one condition was fit for the story condition, and the other

271   condition was fit to the math condition. For the motor task, six conditions were fit: (1) cue; (2)

272   right hand trials; (3) left hand trials; (4) right foot trials; (5) left foot trials; (6) tongue trials. For

273   the relational reasoning task, one condition was fit to trials when the sets of objects were matched,

274   and the other condition was fit to trials when the objects were not matched. For the social cognition

275   task, one condition was fit if the objects were interacting socially (theory of mind), and the other

276   condition was fit to trials where objects were moving randomly. Lastly, for the working memory

277   task, 8 conditions were fit: (1) 2-back body trials; (2) 2-back face trials; (3) 2-back tool trials; (4)

278   2-back place trials; (5) 0-back body trials; (6) 0-back face trials; (7) 0-back tool trials; (8) 0-back

279   place trials. Since all tasks were block designs, each time point for each block was modeled

280   separately for each task condition (i.e., FIR model), with a lag extending up to 25 TRs after task

281   block offset.

282   **fMRI: Task activation**

283   We performed a task GLM analysis on fMRI task data to estimate evoked brain activity

284   during task states. The task timing for each of the 24 task conditions was convolved with the SPM

285   canonical hemodynamic response function to obtain task-evoked activity estimates (Friston et al.,

286   1994). FIR modeling was not used when modeling task-evoked activity. Coefficients were

287   obtained for each parcel in the Glasser et al. (2016) cortical atlas for each of the 24 task conditions.

288   **fMRI: Functional connectivity (FC) estimation**

289   Residual timeseries from the rest and task nuisance regressions were used to estimate

290   functional connectivity for each task. Connectivity values were estimated using zero-lag Pearson

291   product-moment correlations. Timeseries were concatenated across separate runs of the same task

292   to yield a single connectivity value per edge for a given task or resting state condition. For each

293   task scan, we utilized TRs that corresponded to "on-task" timepoints. For instance, we extracted

294   TRs from the working memory scan during N-back task blocks, excluding TRs from the inter-

295   block fixation periods. For the number of TRs included in the connectivity estimates for each

296   condition and scan state, see Table S1.

297   **fMRI: Factor analysis model of latent FC**

298   Factor analysis for obtaining latent FC was conducted with the same approach used to

299   obtain factor scores for generalized intelligence. FC estimates from each separate fMRI task were

300   used as indicators on a unitary factor model and factor scores were obtained using the regression

301   method in the *psych* R package. A separate model was computed for each edge in the connectivity

302   adjacency matrix. We took several approaches to test the predictive utility of latent FC for

303   activation and behavior (detailed below).

304   The first set of analyses tested two alternative measurement approaches for latent FC. The

305   first was to utilize all available data from each functional scan to estimate factor scores for each

306   edge. However, because of the differential amount of scan time for different functional runs (e.g.,

307   ~58 minutes of resting-state versus ~10 minutes of working memory scans), we might expect

308   indicators (i.e., scan types) with more data would dominate the measurement model in the factor

309   analysis. To control for this potential confound, we ran additional analyses where indicators were

310   constrained to have equivalent numbers of TRs used to estimate individual scan functional edges

311   between task and rest, and between different task states. The reasoning task had the fewest "on-

312   task" TRs (264) and therefore served as the limiting factor for task scans data. As such, 264 TRs

313   of each task (for 2112 TRs of task) and a corresponding 2112 TRs of rest were used in these

314   analyses. All of these analyses were performed modeling all available scan types in the same factor

315   model.

316   For activity flow mapping (ActFlow) analyses (Cole et al., 2016; Ito et al., 2020), where

317   activations in held-out regions were predicted using estimated activity flowing over estimated

318   connections, latent FC was estimated independently for each connection by applying leave-one-

319   state-out factor analysis (LOSO-FA) on the state FC estimates to prevent circularity in the

320   predictive model. For instance, when predicting activation in the emotion task, FC estimates were

321   obtained without including the emotion task as an indicator in the factor model.

322

323   **Results**

324   **Factor analysis model of latent connectivity**

325   We ran independent factor analysis models for each connection, estimating the factor

326   loadings of the latent variable (i.e., latent FC) onto each state. Latent FC captures the shared

327   variance in FC across all states (see Figure 2). Factor analyses were run using all available data

328   (i.e., the full time series and all states).

329
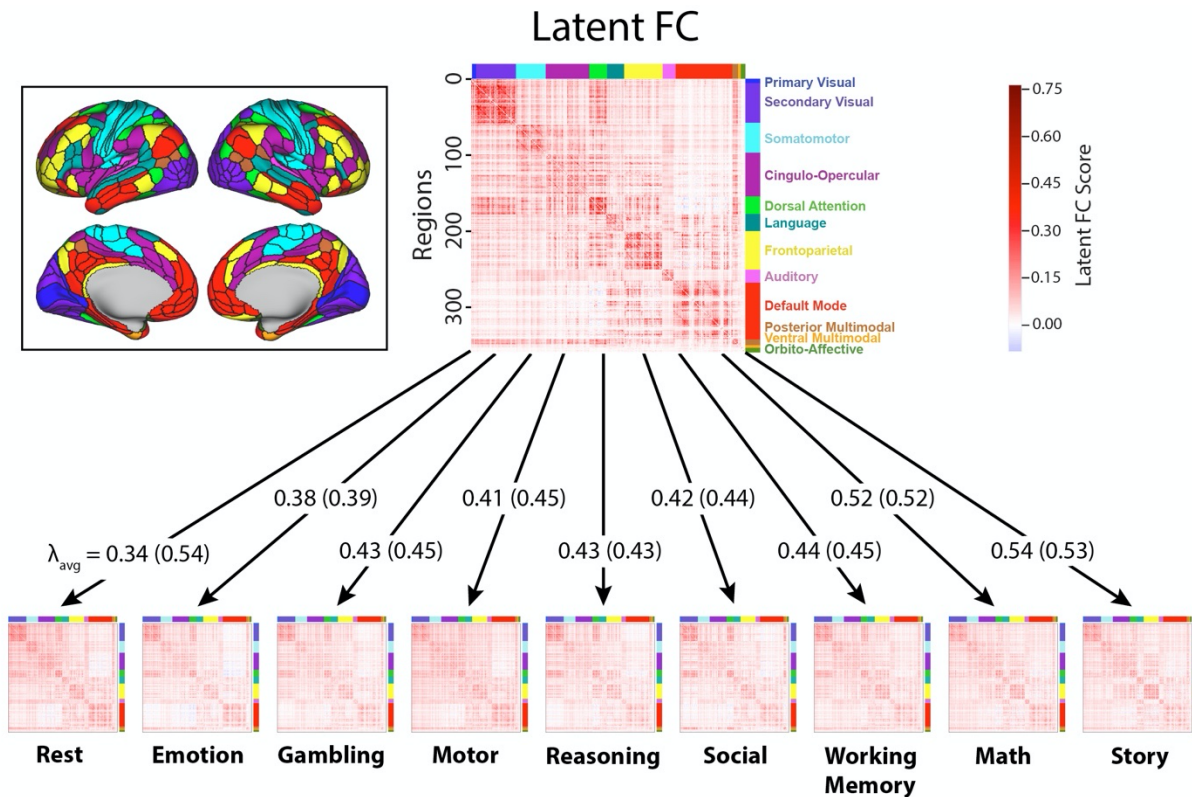
Figure 2. Factor analysis model of latent FC. *Visualization of the latent connectivity matrix and state-specific functional connectivity matrices (group average across subjects). Color along the axes of each matrix corresponds to the network membership of each ROI. For each arrow, the average loadings (λ_{avg}) for each state are shown for analyses controlling for number of TRs (first) and when not controlling for TRs (in parentheses). The averaging loadings for the task states were largely stable across analyses, but the average loading for resting-state increased substantially (from 0.34 to 0.54) when not controlling for the number of TRs. The amount of resting-state data per participant went from 4800 TRs (58 minutes) to 2112 TRs (25 minutes) when matching the total amount of "on-task" time. The network mapping is shown in the cutout (left). Elements in the state-specific matrices represent correlations (r) between regional time series and elements in the latent FC matrix represent factor scores computed from the model for each connection.*

Consistent with our hypothesis that there is a "positive manifold" demonstrating a common latent FC architecture across states, almost all factor loadings were positive (greater than 99%) across all connections and all states (see Table 1). Furthermore, 70.7% of all factor loadings were reasonably large in magnitude (factor loading ≥ 0.4) and 97.4% of connections had two or more states with factor loadings ≥ 0.4 in the full latent FC model. The emotion task had the fewest large factor loadings (47.3%) and the resting state had the most (92.6%) (see Table 1 for full details).

To control for differences between states in the amount of data used to obtain state-specific FC estimates, factor analyses were re-run while matching the number of time points from rest and

350   task data (2112 TRs from rest and 264 TRs for each of the 8 tasks). With this approach, resting

351   state had the fewest number of relatively high magnitude factor loadings of all states – only 31.6%

352   of resting state connections had factor loadings ≥ 0.4. Thus, resting state had the highest factor

353   loadings onto latent FC when a large amount of data was used to estimate resting-state FC, but the

354   lowest factor loadings when less data was used. Controlling for the number of time points between

355   task and rest led to less pronounced changes in the factor loadings of the other states (see Figure

356   2). Note that this drop occurs even though rest continues to have substantially more TRs (8x) than

357   any given task state in these analyses.

State	All Data		Controlling for # Timepoints	
	% Loadings ≥ 0	% Loadings ≥ 0.4	% Loadings ≥ 0	% Loadings ≥ 0.4
Rest	99.9%	92.6%	99.0%	31.6%
Emotion	99.3%	47.3%	98.7%	46.3%
Gambling	99.6%	65.0%	99.1%	62.2%
Motor	99.8%	68.0%	99.4%	54.8%
Reasoning	99.5%	62.1%	99.1%	62.3%
Social	99.8%	66.2%	99.3%	58.4%
Working Memory	99.7%	67.0%	99.2%	64.9%
Math	99.9%	82.4%	99.6%	82.4%
Language	99.9%	86.0%	99.7%	86.3%

358   ***Table 1: Factor Loadings.*** *Almost all factor loadings were positive regardless of whether all resting state data were*
359   *used (left) or we controlled for the number of time points between task and rest (right). Only resting state showed a*
360   *substantial shift in the percent of factor loadings ≥ 0.4 when controlling for the number of timepoints. The amount of*
361   *resting-state data per participant went from 4800 TRs (58 minutes) to 2112 TRs (25 minutes) when matching the total*
362   *amount of "on-task" time.*
363

364   **Latent FC improves generalization to connectivity of held-out states**

365   We next sought to test our second hypothesis: A more reliable and generalizable measure

366   of "intrinsic" connectivity can be estimated by combining information across task states, such as

367   in the factor model, than by using resting state data alone (the current field standard). To test

368   whether the measures of intrinsic FC persist across brain states, we quantified the

369   generalizability of rest FC and latent FC to held-out brain states. To calculate the similarity of

370   FC patterns (i.e., across 64,620 network connections), we computed the Pearon's correlation of

371   rest FC or latent FC with state FC for each individual subject, applying Bonferroni correction to

372   correct for multiple comparisons. For latent FC, similarity was always computed for the state that

373   was held-out while running the factor analysis model. Compared to rest FC, we found that latent

374   FC exhibited significantly greater similarity with a variety of independent brain states (see

375   Figure 3A). Similarity of each state with latent FC was comparable across states, exhibiting the

376   greatest similarity to the WM task ($r = 0.71$) and the least similarity to the social task ($r = 0.66$)

377   and resting state ($r = 0.65$). Rest FC exhibited the greatest similarity to resting state ($r = 0.73$),

378   providing a measure of test-retest similarity of rest FC. For the task states, rest FC had the

379   greatest similarity to the motor task ($r = 0.61$) and the least similarity to the relational task ($r =$

380   0.56).

381   When using the full timeseries (i.e., not controlling for the amount of data used to obtain the FC

382   estimates across states), we still found greater similarity of latent FC relative to rest FC with the

383   task states. However, latent FC exhibited the greatest similarity to the resting state ($r = 0.80$) and

384   the least similarity to the social task ($r = 0.67$; see Figure 3B). Alongside greater similarity

385   estimates with all states, this suggests that states may converge towards latent FC as we sample

386   substantially more data for any given state (e.g., for resting-state FC, 26 minutes of data per

387   participant were included in the data-restricted analysis vs. 58 minutes of data in the unrestricted

388   analysis). All findings were replicated in the validation dataset (Figure S1).

389
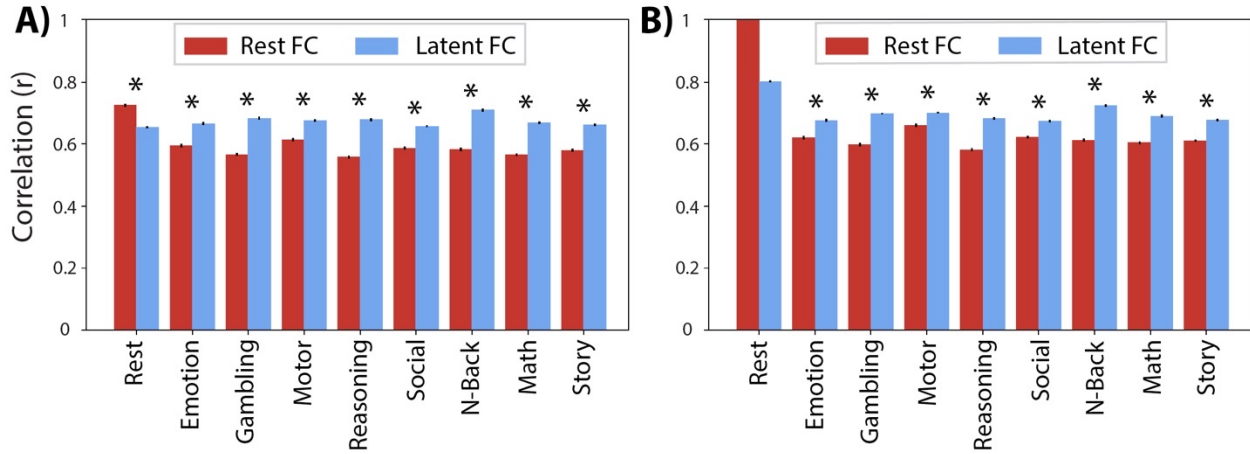
Figure 3. Generalizability of FC patterns. *Pearson's correlation was used to quantify the similarity of latent FC (blue) and rest FC (red) to held-out state FC. Error bars show the standard error of the mean. Asterisks indicate significant differences in similarity of latent FC and rest FC to held-out state FC. A) Results when controlling for the number of time points in the resting state data. This included 25 minutes of resting-state fMRI data, matching the total amount of "on-task" time across all tasks. B) Results when not controlling for the number of time points (including 58 minutes of resting-state data); the resting state prediction is therefore a perfect reproduction (no error bars or comparison). These results are consistent with resting-state FC overfitting to resting state, reducing its generalizability relative to latent FC.*

Latent FC improves prediction of task activation patterns

We next sought to further test our hypothesis that latent FC is highly generalizable (relative to resting-state FC), this time by testing for generalization beyond FC to patterns of task-evoked activation. We began by using GLMs to estimate the pattern of task-evoked activation for each of 24 task conditions. We then used activity flow mapping (Figure. 4A) to predict the pattern of task-evoked activation based on a simple neural network model parameterized using either resting-state FC or latent FC. We used Pearson's correlation to compute the similarity of predicted-to-actual task activations of two activity flow models with different connectivity estimates based on either latent FC or rest FC. As a global measure of performance, we first correlated the predicted activation patterns from the activity flow model using rest and latent FC with the observed activations. Predicted activation patterns from activity flow models with connectivity based on latent FC ($r = 0.66$) outperformed predictions based on resting state FC ($r = 0.56$) in reproducing the observed beta activation patterns. We then compared the results of the two models at the region

413   (i.e., prediction for a given region across conditions) and condition (i.e., prediction for a given

414   condition across regions) level.

415   We first estimated predicted beta activations for each region (across conditions) using the

416   activity flow models. This reflects the changes in activation within each region that are dependent

417   on the task condition. For each region, we compared the beta activation predictions of the two

418   activity flow models. For each network, we computed the percent of regions with significantly

419   improved predictions for one of the two models. When using the activity flow model based on

420   latent FC, the predictions were significantly improved for 68% of brain regions (246 out of 360

421   total), accounting for 33% of VIS1, 69% of VIS2, 64% of SMN, 73% of CON, 70% of DAN, 62%

422   of LAN, 62% of FPN, 100% of AUD, 78% of DMN, 14% of PMM, 0% of VMM, and 33% of

423   ORA. Activity flow based on rest FC significantly improved predictions in 1% of brain regions (4

424   out of 360 total), accounting for 7% of VIS2 and no other networks (Figure 4B).

425   When considering prediction accuracy for each task condition, we found that latent FC

426   significantly improved the across-region predicted activations for all task conditions – except the

427   left-hand condition of the motor task – when comparing the relative activations across the topology

428   of the brain within a condition (Figure 4C). Overlap of predicted-to-actual task activations for the

429   activity flow models were variable by task condition. The activity flow model based on latent FC

430   exhibited the greatest similarity to the 2-back body condition of the WM task ($r = 0.76$) and the

431   least similarity to the math condition of the language task ($r = 0.45$). The activity flow model based

432   on rest FC exhibited the greatest similarity to the matching condition of the relational task ($r =$

433   0.67) and the least similarity to the math condition of the language task ($r = 0.4$). All findings were

434   replicated in the validation dataset (Figure S2).

435
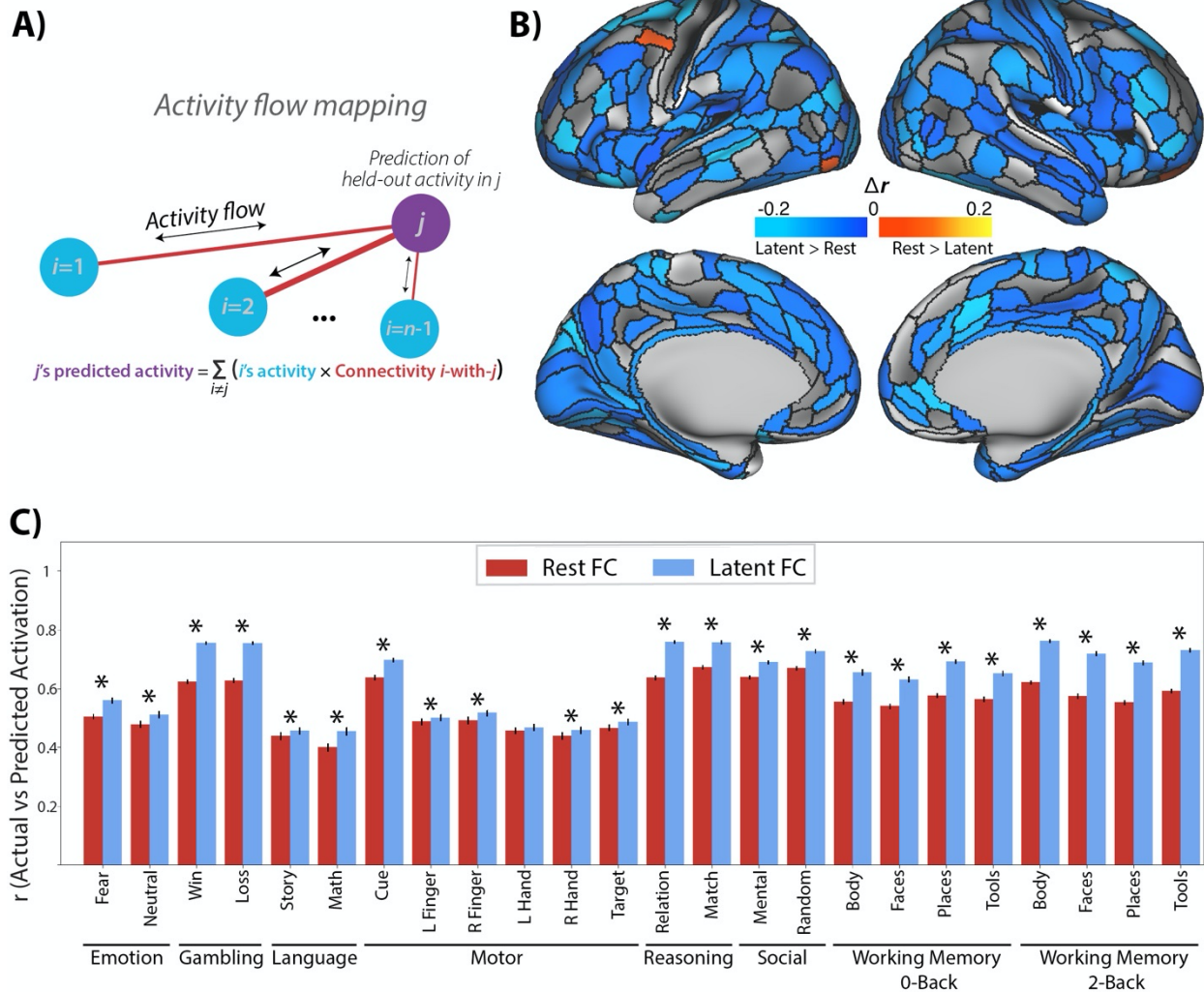
Figure 4. Comparison of activity flow models based on latent FC versus rest FC. *A) Conceptual model of the activity flow mapping algorithm (Cole et al., 2016) which models the activity of a held-out region (*j*) as the sum of activity in other brain regions (*i*) weighted by their shared functional connectivity (*ij*).* ***B)*** *Task activation prediction accuracies by region. Regions with prediction accuracies that were significantly greater using the activity flow model based on latent FC shown in cool colors. Regions with prediction accuracies that were significantly greater using the activity flow model based on rest FC shown in warm colors. The vast majority of regions showing a significant difference showed prediction advantages for latent FC.* ***C)*** *Task activation prediction accuracies by condition. Pearson's correlation was used to quantify the similarity of predicted-to-actual task activations using activity flow models with connectivity based on either rest FC (*red*) or latent FC (*blue*). Error bars show the standard error of the mean correlation. Asterisks indicate significant differences in similarity of beta activations from models based on latent FC versus rest FC.*

**Latent FC improves prediction of general intelligence**

Our hypothesis that latent FC generalizes better than resting-state FC also predicts that latent FC should be more related to general cognition and behavior, even behavior independent of

452   the particular tasks used for estimating the task-state FC going into the latent FC estimates. We

453   tested whether latent FC improves prediction of general intelligence using psychometric g to

454   capture many different behavioral and cognitive measures (Dubois, Galdi, Paul, & Adolphs, 2018;

455   Gottfredson, 1997). We estimated general intelligence (psychometric g) using a factor analysis

456   model on behavioral data from a range of cognitive tasks, then tested whether latent FC and/or rest

457   FC measures could predict general intelligence. We combined the exploration and validation

458   samples to increase the number of participants to 352 for this analysis, given the need for additional

459   participants (relative to the other analyses in this study) to achieve reasonable statistical power for

460   individual difference correlations (Yarkoni, 2009). We employed multiple linear regression to

461   predict general intelligence from FC, implementing a leave-one-subject-out cross-validation

462   approach to avoid analysis circularity (Dubois et al., 2018).

463   We found that predicted general intelligence was significantly correlated with actual

464   general intelligence for models using both rest FC ($r = 0.33$, $p = 3.19e-10$) and latent FC ($r = 0.45$,

465    $p = 1.28e-18$) (Figure 5A). Consistent with our hypothesis, the model using latent FC significantly

466   improved prediction of general intelligence compared to the model using rest FC ($\Delta r = 0.12$, $t =$

467   2.33, $p = 0.01$, see Eid et al., 2011 for correlation comparison method). The magnitude of this

468   effect was large, as the percent linear variance explained by latent FC ($r^2 = 0.200$) was almost two

469   times the percent linear variance explained by rest FC ($r^2 = 0.107$). In comparison with the overall

470   sample results, the correlation and difference in R^2 was substantially larger for the exploratory

471   sample (Figure 5B) while the validation set showed a more-similar difference in R^2 despite lower

472   correlations between predicted and actual psychometric g scores for both latent and rest FC data

473   (Figure 5C). A meta-analysis of the exploratory and validation samples suggested that the pooled

474   correlation difference effect was significant ($\Delta z_{pooled} = 0.19$, $p < 0.001$)

475
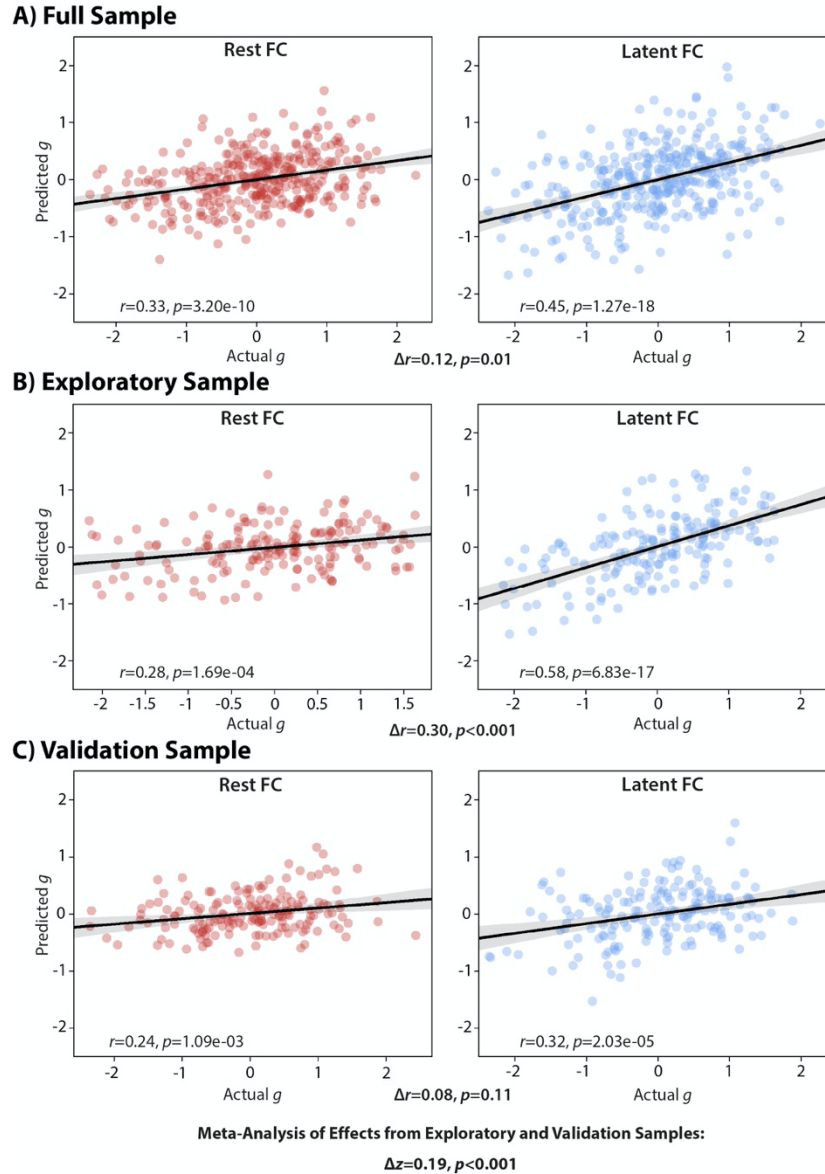
Figure 5. Relationship between actual and predicted general intelligence. *Results of multiple linear regression models from rest FC and latent FC in the **A)** overall, **B)** exploratory, and **C)** validation sample. The significance of the difference in correlation (Δr) is indicated below each plot. A meta-analysis of the exploratory and validation samples showed a significant difference in the correlations between actual and predicted g scores when comparing rest to latent FC (Δz = 0.19, p < 0.001).*

Comparing latent and average FC

While the factor model uses the covariance among the different states to compute optimal

weights, a simpler approach to finding consensus among states involves taking a simple average

486   across states. This approach assumes the weights/loadings between measured states are equal.

487   Given that the computed weights in our results with latent FC were relatively uniform across states,

488   we determined that this assumption was reasonable in this case. This supports the use of average

489   FC, however we directly compared latent FC to average FC to assess whether there were any

490   advantages to either method. To compare the factor model with a simple average, we computed

491   the mean value of each edge across states to construct an average connectivity matrix. For all

492   analyses, we controlled for the amount of data between rest and task. Results indicated that

493   combining across states, regardless of the approach, shows substantial improvements over using

494   even the full resting state data. Indeed, the average FC approach appears to out-perform the latent

495   FC approach (albeit only slightly) in generalizing to held-out connectivity states (Figure 6A). In

496   the activity flow mapping results, however, latent FC consistently outperforms average FC in

497   predicting regional activity patterns, showing better predictions in 348 out of 360 regions (97%),

498   whereas average FC showed no improved predictions (Figure 6B). Similarly, latent FC

499   outperformed average FC in condition-wise activity flow predictions in 22 out of 24 conditions

500   (Figure 6C). Together these results suggest that the average FC approach (sometimes termed

501   "general functional connectivity") is a reasonable alternative to the more complex latent FC

502   approach, so long as the optimal weights across states are close to equal (an assumption not made

503   by latent FC). This difference between the methods would likely become more meaningful in cases

504   wherein a particular brain state is highly distinct from all others (e.g., deep sleep vs. conscious

505   states) or when one or more states is much noisier than the others (which would be weighted lower

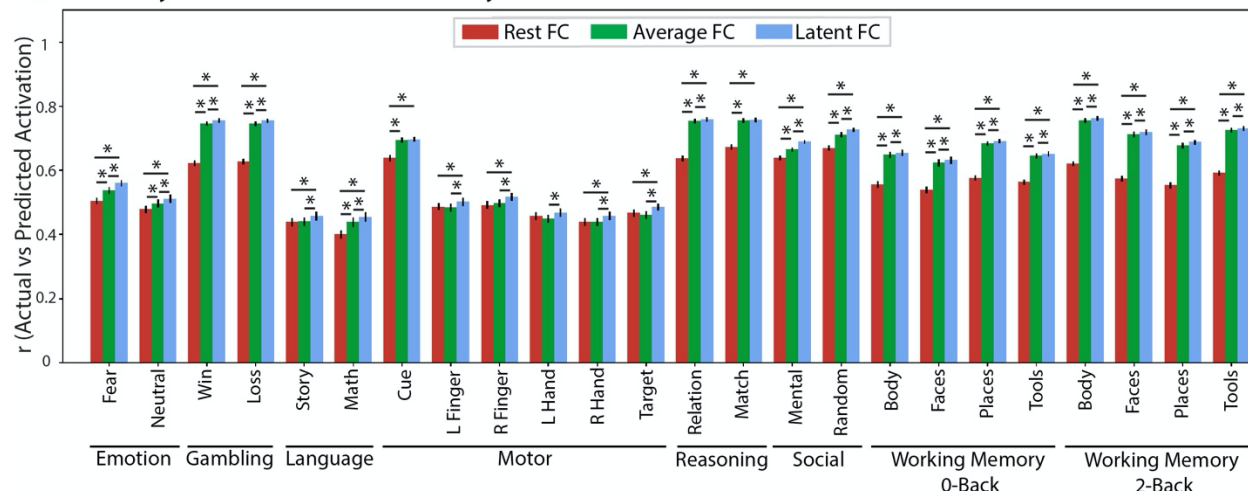506   by latent FC but not average FC).

507

A) Generalizing Connectivty
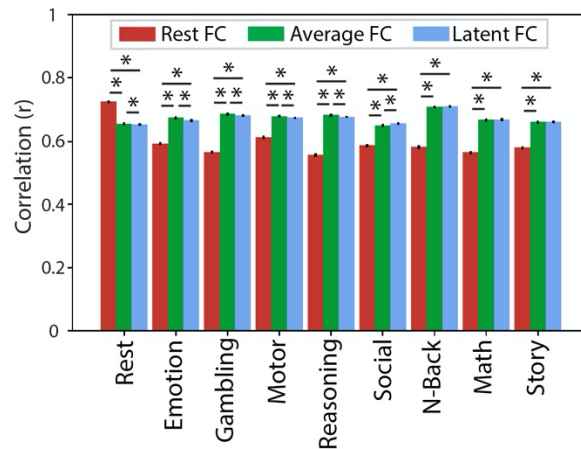
B) Activity Flow Predictions: by region
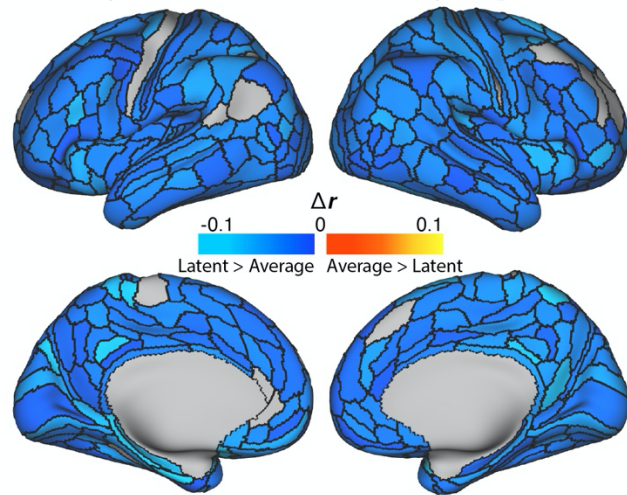
C) Activity Flow Predictions: by condition

508
509 *Figure 6. Comparison of A) Generalizing connectivity and B) Activity flow models by region and C) condition,*
510 *based on latent FC and average FC versus Rest. A) Both average (green) and latent (blue) FC outperformed rest*
511 *FC on generalizing to all task states except resting state. Average FC performed similarly or slightly better than*
512 *latent FC on all held-out states (asterisks denote significant differences, the higher position represents the test of*
513 *rest vs latent FC). B) In contrast, latent FC outperformed average FC in predicting task activation in 97% of*
514 *regions, whereas average FC outperformed in 0% regions. C) Across all conditions, latent FC was a better*
515 *predictor than average FC of held-out activations (lower asterisks indicate significant difference between adjacent*
516 *bars; higher asterisks indicate significant difference between latent and rest FC). All results control for the number*
517 *of time points in the resting state data.*
518

519 **Discussion**

520   Defining a map of task-independent, intrinsic functional connections in the brain is a major

521 aim of basic research in cognitive neuroscience. Intrinsic FC persists across task states, making it

522 a more reliable and generalizable measure of the underlying functional dynamics that shape

523   cognition and behavior. As such, measures of intrinsic FC are better candidates to serve as stable

524   biomarkers of important individual differences in behavioral outcomes (M. Elliott et al., 2019).

525   We utilized a factor analytic approach, a well-developed technique from measurement

526   psychometrics (Bollen, 2002), to define intrinsic FC as a latent variable derived from the common

527   variances in FC across task states. We compared the factor model against the standard approach

528   applied in the field, FC derived from resting state. The factor model not only shows enhanced

529   measurement and predictive properties beyond measures of intrinsic FC derived from resting state,

530   it also offers a unique theoretical perspective on the relationship between intrinsic and task-specific

531   brain states. In a latent variable model, individual task states are viewed as observable sample

532   realizations of the underlying intrinsic connectivity, and task-specific deviations from this baseline

533   are modeled as unique errors arising from a combination of noise and state-specific properties. The

534   factor modeling approach allows researchers to not only gain traction in defining intrinsic FC

535   common among brain states, but also to separate and explore properties that are specific to

536   individuals and states.

537   **Factor Analytic Model of Functional Connectivity**

538   　　We began by building factor analysis models of latent FC using two approaches. In the

539   first, we modeled latent FC using all available data. In this model, resting state functional

540   connections had the highest number of significant loadings of any condition. However, when

541   controlling for the number of time-points (by reducing the number of resting state timepoints to

542   match the tasks with shorter durations), resting state connections had the lowest percentage of

543   significant factor loadings. This property of the factor model highlights one of its strengths; higher

544   precision measurements show higher fidelity to the underlying common latent factor than lower-

545   precision measures. Here, the precision appears to be driven primarily by the amount of data.

546 However, in the absence of stringent data quality control, the factor model can also down-weight

547 poor-quality data (e.g., high motion, artifacts) relative to higher-quality data when variability

548 associated with noise does not replicate across task states.

549 Conversely, tasks that more closely represent underlying intrinsic FC will show stronger

550 factor loadings, similar to how the Raven's Progressive Matrices task loads highly onto the

551 generalized intelligence factor (Dubois et al., 2018). Given its widespread use as a marker of

552 intrinsic FC, we might have expected that resting state would load highly onto the latent FC factor

553 regardless of how much data went into its estimation. However, when controlling for the amount

554 of data used to estimate FC, the resting state loadings were lower than all other examined states,

555 even though there were still many more TRs of resting state than any one task state. Additionally,

556 when using the full amount of data to estimate rest FC, the factor loadings for resting state was

557 similar to the story and math tasks, each of which were estimated with much less data (Figure 2;

558 values in parentheses). These results suggest that resting state is not an especially good proxy for

559 intrinsic FC, which aligns with its relatively poor performance compared with latent FC in

560 predicting the patterns of connectivity and evoked brain activity observed for other states.

561 **Latent FC as a Reliable Measure of Intrinsic Connectivity**

562 As mentioned previously, a marker of intrinsic connectivity is its persistence across task

563 states (i.e., generalizability), as well as its ability to accurately recapitulate observed realizations

564 of evoked brain activity and connectivity (M. Elliott et al., 2019; M. L. Elliott et al., 2020; Kragel,

565 Han, Kraynak, Gianaros, & Wager, 2020; Parkes, Satterthwaite, & Bassett, 2020). Our results

566 highlight the advantages of latent versus rest FC to reliably predict independent connectivity and

567 regional activations. When comparing patterns of connectivity, we showed that latent FC showed

568 higher correlation with held-out, task-specific connectivity states compared with rest FC, with the

569   sole exception of resting state connectivity where rest FC outperformed. This pattern of results

570   suggests that resting state FC is less generalizable as a measure of intrinsic connectivity and instead

571   there are resting state-specific factors which shape the dynamics of rest FC that are not present in

572   other states.

573   One potential explanation for this might be that tasks as a group reliably differ from rest FC's more

574   intrinsic profile, and the reduction in generalizability reflects deviations from a default state. Under

575   this explanation, the latent FC advantage could simply reflect that there are more task indicators

576   in the measurement model than rest (although note that even when controlling for number of

577   timepoints, the amount of rest data is equal to all the tasks combined) and we would predict that

578   latent FC would be a poorer representation of rest FC patterns of connectivity. However, results

579   did not show a substantial drop in the correlation of latent and rest FC compared to the correlations

580   of latent FC with the various task FC patterns (blue bars, Figure 3). Indeed, it is rest FC that shows

581   a drop in performance in its correlations with resting state versus task connectivity, suggesting that

582   latent FC does a better job of representing common, stable variability in FC profiles across both

583   rest and task states. Importantly, latent FC does so even though the task or rest condition being

584   correlated is left out of the factor model for that specific comparison to avoid circularity. As such,

585   the factor score analytically has different indicators across all comparisons, and nevertheless still

586   outperforms rest FC. Moreover, obtaining a better sample of the resting state by using the full time

587   series resulted in the resting state having the highest factor loadings and a strongest correlation

588   with latent FC, which suggests that over time the resting state converges to latent FC.

589

590   The advantages of latent FC are not, however, restricted to the connectivity space; the latent

591 measure of intrinsic FC also outperforms rest FC in predicting state-specific activation patterns.

592 Not only did latent FC support higher prediction accuracy by the activity flow model of task

593 activation globally (r_{latent} = 0.66 vs. r_{rest} = 0.56), it showed condition-specific advantages in 23 out

594 of 24 specific task conditions (Figure 4B). Rest FC, in comparison, displayed higher prediction

595 accuracy in none of the task conditions (in the left-hand motor condition, latent and rest FC

596 performed comparably; Figure 4C). When we examined predictions of region-specific patterns of

597 activation, results showed that latent FC had improved prediction over rest FC for 68% of all brain

598 regions across a variety of distributed networks. In contrast, rest FC showed improved prediction

599 for only 1.1% of regions, all of which were restricted to the VIS2 network (and constituted only

600 7% of that network). These improvements, as before, were not due to circularity in the analyses,

601 as task predictions using latent FC were done using the leave-one-task-out approach in the factor

602 model.

603 **Improving External Validity with Latent FC**

604   While latent FC has demonstrable advantages for prediction within the brain, its utility as

605 a method of estimating brain-based biomarkers relies on its predictive validity for outcomes of

606 interest. Here, we showed that connectivity values from latent FC showed superior prediction of a

607 metric of generalized intelligence (psychometric *g*) than did rest FC connections. Although both

608 rest FC and latent FC values significantly predicted individual differences in generalized

609 intelligence, latent FC doubled the percent of explained variance in the outcome over rest FC (20%

610 versus 10%). In measurement science, this is a hallmark advantage of the latent variable approach

611 used in factor analysis. Methods which fail to account for measurement error tend to show reduced

612 relationships between variables, whereas modeling state-specific error terms dis-attenuates those

613   relationships (Schmidt & Hunter, 1996). Indeed, generalized intelligence is generally modeled

614   with a factor analytic approach for precisely this reason. We demonstrate that the framework for

615   improving measurement properties in behavioral measures applies equally to measures derived

616   from functional neuroimaging data. As such, factor analytic models are ideal for aiding the search

617   for biomarkers across a wide domain of individual difference outcomes.

618   **State Aggregation Improves Predictive Performance**

619   The performance of average FC suggests that aggregating information across states has

620   advantages over longer scan sessions of resting state, regardless of the approach used.

621   Interestingly, average FC performance is not uniform in relation to the latent FC, performing as-

622   good or slightly better than latent FC in correlating with state-specific connectivity, but

623   underperforming latent FC in predicting held out activity in almost all regions. A few

624   circumstances may predict when we would expect to see more or less pronounced differences

625   between average and latent FC. First, data quality: We expect more pronounced differences for

626   lower quality data and less pronounced differences for higher quality data. The HCP data used

627   here is of extremely high quality, which reduces variability in noise between scans. This is

628   reflected in the average factor loadings which are relatively close in value across states (Figure 2).

629   Of course, as the loadings converge in value, the more similar average and latent FC will become

630   (here the connectivity values are correlated; $r = .98$). Second, the method of factor analysis used:

631   Here, we opted to fit a single-factor model for each connection independently due to the large

632   number of operations (e.g., separate models for each connection). However, a single factor in

633   isolation may not be the best fit for brain data (van Kesteren & Kievit, 2020) and the method here

634   might represent a sort of floor performance for latent FC relative to approaches which adopt a

635   dependent model that tries to optimize the fit for each factor model.

636   Finally, there appear to be differences depending on the type of dependent variable in

637 question. For example, while the factor and average models converge in their correlation with

638 connectivity for held-out states, we found that activity flow models that incorporated latent FC

639 performed better. Average and factor models produced similar patterns of relative connectivity

640 (i.e., highly correlated patterns of FC), however the distribution of connectivity values differ.

641 Latent FC estimates exhibited a sparser distribution of connectivity by zero-ing out low and/or

642 unstable connections, which may have improved the activity flow models by reducing the

643 contributions of disconnected brain regions (see Figure S4).

644   Despite the relatively small differences in performance between average and latent FC,

645 there are theoretical reasons to prefer a latent variable perspective for FC estimation. The first, as

646 mentioned before, is that while the average FC must assume equal loadings, latent FC makes this

647 a testable hypothesis. If loadings converge towards equal values, then average and latent FC will

648 converge (as they nearly did here). This suggests that averaging will likely perform well under

649 conditions similar to the HCP data (high quality, young adult data). However, as the data diverges

650 from this baseline, latent FC should have advantages by weighting data according to how closely

651 it reflects intrinsic functional states and contributes to the common variance across measures. If

652 differences among measures increase (i.e., measures reflect intrinsic FC better or worse), we would

653 hypothesize that average and latent FC would diverge in their performance. However, apart from

654 these practical considerations, a latent variable model of FC is a good theoretical model for how

655 state-specific functional connections emerge from underlying, intrinsic neural connectivity.

656 Intrinsic connectivity is an unobserved state (Bollen, 2002) that gives rise to state specific

657 phenotypes based on combinations of common (i.e., the latent factor) and state-specific (i.e., the

658 error) variance.

Conclusions

659

660   In summary, we utilized a factor analytic approach to derive intrinsic FC from multiple

661   task and resting state data. Our derived measure, termed latent FC, showed improved

662   generalizability and reliability compared to a standard measure of resting-state FC. Not only did

663   latent FC do a better job of reflecting state-specific FC patterns across tasks, it also

664   overwhelmingly improved predictions of regional activations when utilized in activity flow

665   models. Finally, connectivity derived from latent FC doubled the predictive utility of an external

666   measure of generalized intelligence (g) compared with connectivity from rest FC, highlighting its

667   suitability for use in clinical and other individual difference research, where reliable biomarkers

668   are needed. These results present compelling support for the use of factor analytic models in

669   cognitive neuroscience, demonstrating the value of established tools from psychometrics for

670   enhancing measurement quality in neuroscience.

671
672

Author contributions

KLA and MWC designed the analytic approach. EMM and KLA carried out analyses with MWC. EMM, KLA, and MWC wrote the manuscript, with feedback received from all other authors.

Conflict of interest

The authors declare no competing financial interests.

692 **References**

693 Anderson, J. S., Ferguson, M. A., Lopez-Larson, M., & Yurgelun-Todd, D. (2011).

694   Reproducibility of single-subject functional connectivity measurements. *AJNR. American*

695   *Journal of Neuroradiology*, *32*(3), 548–555.

696 Barch, D. M., Burgess, G. C., Harms, M. P., Petersen, S. E., Schlaggar, B. L., Corbetta, M., …

697   WU-Minn HCP Consortium. (2013). Function in the human connectome: task-fMRI and

698   individual differences in behavior. *NeuroImage*, *80*, 169–189.

699 Behzadi, Y., Restom, K., Liau, J., & Liu, T. T. (2007). A component based noise correction

700   method (CompCor) for BOLD and perfusion based fMRI. *NeuroImage*, *37*(1), 90–101.

701 Bollen, K. A. (2002). Latent variables in psychology and the social sciences. *Annual Review of*

702   *Psychology*, *53*, 605–634.

703 Ciric, R., Wolf, D. H., Power, J. D., Roalf, D. R., Baum, G. L., Ruparel, K., … Satterthwaite, T.

704   D. (2017). Benchmarking of participant-level confound regression strategies for the

705   control of motion artifact in studies of functional connectivity. *NeuroImage*, *154*, 174–

706   187.

707   Cohen, M. R., & Kohn, A. (2011). Measuring and interpreting neuronal correlations. *Nature*

708   *Neuroscience*, *14*(7), 811–819.

709   Cole, M. W., Bassett, D. S., Power, J. D., Braver, T. S., & Petersen, S. E. (2014). Intrinsic and

710   task-evoked network architectures of the human brain. *Neuron*, *83*(1), 238–251.

711   Cole, M. W., Ito, T., Bassett, D. S., & Schultz, D. H. (2016). Activity flow over resting-state

712   networks shapes cognitive task activations. *Nature Neuroscience*, *19*(12), 1718–1726.

713   Cole, M. W., Ito, T., Schultz, D., Mill, R., Chen, R., & Cocuzza, C. (2019). Task activations

714   produce spurious but systematic inflation of task functional connectivity estimates.

715   *NeuroImage*, *189*, 1–18.

716   Dubois, J., Galdi, P., Paul, L. K., & Adolphs, R. (2018). A distributed brain network predicts

717   general intelligence from resting-state human neuroimaging data. *Philosophical*

718   *Transactions of the Royal Society of London. Series B, Biological Sciences*, *373*(1756).

719   doi:10.1098/rstb.2017.0284

720   Elliott, M., Knodt, A., Cooke, M., Kim, J., Melzer, T., Keenan, R., … Hariri, A. (2019). S7.

721   General functional connectivity: Shared features of resting state and task fMRI drive

722   reliable and heritable individual differences in functional brain networks. *Biological*

723   *Psychiatry*, *85*(10), S299.

724   Elliott, M. L., Knodt, A. R., Ireland, D., Morris, M. L., Poulton, R., Ramrakha, S., … Hariri, A.

725   R. (2020). What Is the Test-Retest Reliability of Common Task-Functional MRI

726 Measures? New Empirical Evidence and a Meta-Analysis. *Psychological Science*, *31*(7),

727 792–806.

728 Fox, M. D., & Raichle, M. E. (2007). Spontaneous fluctuations in brain activity observed with

729 functional magnetic resonance imaging. *Nature Reviews. Neuroscience*, *8*(9), 700–711.

730 Friston, K. J., Holmes, A. P., Worsley, K. J., Poline, J.-P., Frith, C. D., & Frackowiak, R. S. J.

731 (1994). Statistical parametric maps in functional imaging: A general linear approach.

732 *Human Brain Mapping*, *2*(4), 189–210.

733 Gershon, R. C., Wagster, M. V., Hendrie, H. C., Fox, N. A., Cook, K. F., & Nowinski, C. J.

734 (2013). NIH Toolbox for Assessment of Neurological and Behavioral Function.

735 *Neurology*, *80*(11 Supplement 3), S2–S6.

736 Glasser, M. F., Coalson, T. S., Bijsterbosch, J. D., Harrison, S. J., Harms, M. P., Anticevic, A.,

737 … Smith, S. M. (2018). Using temporal ICA to selectively remove global noise while

738 preserving global signal in functional MRI data. *NeuroImage*, *181*, 692–717.

739 Glasser, M. F., Coalson, T. S., Robinson, E. C., Hacker, C. D., Harwell, J., Yacoub, E., … Van

740 Essen, D. C. (2016). A multi-modal parcellation of human cerebral cortex. *Nature*,

741 *536*(7615), 171–178.

742 Gottfredson, L. S. (1997). Mainstream science on intelligence: An editorial with 52 signatories,

743 history, and bibliography. *Intelligence*, *24*(1), 13–23.

744 Gratton, C., Laumann, T. O., Nielsen, A. N., Greene, D. J., Gordon, E. M., Gilmore, A. W., …

745 Petersen, S. E. (2018). Functional brain networks are dominated by stable group and

746 individual factors, not cognitive or daily variation. *Neuron*, *98*(2), 439-452.e5.

747 Gur, R. C., Richard, J., Hughett, P., Calkins, M. E., Macy, L., Bilker, W. B., … Gur, R. E.

748 (2010). A cognitive neuroscience-based computerized battery for efficient measurement

749   of individual differences: standardization and initial construct validation. *Journal of*

750   *Neuroscience Methods*, *187*(2), 254–262.

751 Hacker, C. D., Laumann, T. O., Szrama, N. P., Baldassarre, A., Snyder, A. Z., Leuthardt, E. C.,

752   & Corbetta, M. (2013). Resting state network estimation in individual subjects.

753   *NeuroImage*, *82*, 616–633.

754 Honey, C. J., Sporns, O., Cammoun, L., Gigandet, X., Thiran, J. P., Meuli, R., & Hagmann, P.

755   (2009). Predicting human resting-state functional connectivity from structural

756   connectivity. *Proceedings of the National Academy of Sciences of the United States of*

757   *America*, *106*(6), 2035–2040.

758 Ito, T., Brincat, S. L., Siegel, M., Mill, R. D., He, B. J., Miller, E. K., … Cole, M. W. (2020).

759   Task-evoked activity quenches neural correlations and variability across cortical areas.

760   *PLoS Computational Biology*, *16*(8), e1007983.

761 Kovacs, K., & Conway, A. R. A. (2016). Process overlap theory: A unified account of the

762   general factor of intelligence. *Psychological Inquiry*, *27*(3), 151–177.

763 Kragel, P. A., Han, X., Kraynak, T. E., Gianaros, P. J., & Wager, T. D., Ph. D. (2020). fMRI can

764   be highly reliable, but it depends on what you measure. doi:10.31234/osf.io/9eaxk

765 Krienen, F. M., Yeo, B. T. T., & Buckner, R. L. (2014). Reconfigurable task-dependent

766   functional coupling modes cluster around a core functional architecture. *Philosophical*

767　　　　　*Transactions of the Royal Society of London. Series B, Biological Sciences*, *369*(1653),

768　　　　　20130526.

769　Laumann, T. O., Gordon, E. M., Adeyemo, B., Snyder, A. Z., Joo, S. J., Chen, M.-Y., …

770　　　　　Petersen, S. E. (2015). Functional System and Areal Organization of a Highly Sampled

771　　　　　Individual Human Brain. *Neuron*, *87*(3), 657–670.

772　McNeish, D., & Wolf, M. G. (2020). Thinking twice about sum scores. *Behavior Research*

773　　　　　*Methods*, *52*(6), 2674.

774　Murphy, K., Birn, R. M., Handwerker, D. A., Jones, T. B., & Bandettini, P. A. (2009). The

775　　　　　impact of global signal regression on resting state correlations: are anti-correlated

776　　　　　networks introduced? *NeuroImage*, *44*(3), 893–905.

777　Parkes, L., Satterthwaite, T. D., & Bassett, D. S. (2020). Towards precise resting-state fMRI

778　　　　　biomarkers in psychiatry: synthesizing developments in transdiagnostic research,

779　　　　　dimensional models of psychopathology, and normative neurodevelopment. *Current*

780　　　　　*Opinion in Neurobiology*, *65*, 120–128.

781　Power, J. D., Mitra, A., Laumann, T. O., Snyder, A. Z., Schlaggar, B. L., & Petersen, S. E.

782　　　　　(2014). Methods to detect, characterize, and remove motion artifact in resting state fMRI.

783　　　　　*NeuroImage*, *84*, 320–341.

784　Power, J. D., Plitt, M., Gotts, S. J., Kundu, P., Voon, V., Bandettini, P. A., & Martin, A. (2018).

785　　　　　Ridding fMRI data of motion-related influences: Removal of signals with distinct spatial

786   and physical bases in multiecho data. *Proceedings of the National Academy of Sciences*

787   *of the United States of America*, *115*(9), E2105–E2114.

788 Raichle, M. E. (2006). Neuroscience. The brain's dark energy. *Science (New York, N.Y.)*,

789   *314*(5803), 1249–1250.

790 Revelle, W. R. (2017). *psych: Procedures for Personality and Psychological Research*.

791   Retrieved from https://www.scholars.northwestern.edu/en/publications/psych-

792   procedures-for-personality-and-psychological-research

793 Schmidt, F. L., & Hunter, J. E. (1996). Measurement error in psychological research: Lessons

794   from 26 research scenarios. *Psychological Methods*, *1*(2), 199–223.

795 Smith, S. M., Beckmann, C. F., Andersson, J., Auerbach, E. J., Bijsterbosch, J., Douaud, G., …

796   WU-Minn HCP Consortium. (2013). Resting-state fMRI in the Human Connectome

797   Project. *NeuroImage*, *80*, 144–168.

798 Smith, S. M., Fox, P. T., Miller, K. L., Glahn, D. C., Fox, P. M., Mackay, C. E., … Beckmann,

799   C. F. (2009). Correspondence of the brain's functional architecture during activation and

800   rest. *Proceedings of the National Academy of Sciences of the United States of America*,

801   *106*(31), 13040–13045.

802   Spearman, C. (1904). "General Intelligence" Objectively Determined and Measured. *The*

803   *American Journal of Psychology*, *15*(2), 201–293.

804   Thurstone, L. L. (1935). *The vectors of mind: Multiple-factor analysis for the isolation of*

805   *primary traits*. Retrieved from https://psycnet.apa.org/psycinfo/2004-16228-000/

806   Van Essen, D. C., Smith, S. M., Barch, D. M., Behrens, T. E. J., Yacoub, E., Ugurbil, K., & WU-

807   Minn HCP Consortium. (2013). The WU-Minn Human Connectome Project: an

808   overview. *NeuroImage*, *80*, 62–79.

809   van Kesteren, E.-J., & Kievit, R. A. (2020). Exploratory Factor Analysis with Structured

810   Residuals for Brain Imaging Data (p. 2020.02.06.933689).

811   doi:10.1101/2020.02.06.933689

812   Wong, C. W., Olafsson, V., Tal, O., & Liu, T. T. (2013). The amplitude of the resting-state fMRI

813   global signal is related to EEG vigilance measures. *NeuroImage*, *83*, 983–990.

814   Yarkoni, T. (2009). Big Correlations in Little Studies: Inflated fMRI Correlations Reflect Low

815   Statistical Power-Commentary on Vul et al. (2009). *Perspectives on Psychological*

816   *Science: A Journal of the Association for Psychological Science*, *4*(3), 294–298.